THE JOURNAL OF BIOLOGICAL CHEMISTRY VOL. 288, NO. 50, pp. 36040–36051, December 13, 2013

NAT8L (*N*-Acetyltransferase 8-Like) Accelerates Lipid Turnover and Increases Energy Expenditure in Brown Adipocytes*

Received for publication, June 4, 2013, and in revised form, October 15, 2013 Published, JBC Papers in Press, October 23, 2013, DOI 10.1074/jbc.M113.491324

Ariane R. Pessentheiner[‡§1], Helmut J. Pelzmann[‡§1], Evelyn Walenta[‡], Martina Schweiger[¶], Lukas N. Groschner[‖], Wolfgang F. Graier[‖], Dagmar Kolb[‡‡], Kyosuke Uno[§§], Toh Miyazaki[§§], Atsumi Nitta[§§], Dietmar Rieder[¶¶], Andreas Prokesch[‡§], and Juliane G. Bogner-Strauss[‡§2]**

From the [‡]Institute for Genomics and Bioinformatics, Graz University of Technology, Petergasse 14, 8010 Graz, Austria, the [§]Institute of Biochemistry, Graz University of Technology, Petergasse 12, 8010 Graz, Austria, the [¶]Institute for Molecular Biosciences, University of Graz, Heinrichstrasse 31, 8010 Graz, Austria, the [‖]Institute of Molecular Biology and Biochemistry and [**]Institute of Cell Biology, Histology, and Embryology, Medical University of Graz, Harrachgasse 21, 8010 Graz, Austria, the [‡‡]Core Facility Ultrastructure Analysis, Center for Medical Research, Medical University of Graz, Stiftingtalstrasse 24, 8010 Graz, Austria, the [§§]Department of Pharmaceutical Therapy and Neuropharmacology, Faculty of Pharmaceutical Sciences, Graduate School of Medicine and Pharmaceutical Sciences, University of Toyama, 2630 Sugitani, Toyama 930-0194, Japan, and the [¶¶]Division of Bioinformatics, Biocenter, Innsbruck Medical University, Innrain 80, 6020 Innsbruck, Austria

Background: NAT8L (*N*-acetyltransferase 8-like) synthesizes *N*-acetylaspartate and is required for myelination in the brain. Its function in other tissues was undefined.
Results: *Nat8l* is highly expressed in adipose tissues and impacts adipogenic marker gene expression, lipid turnover, and energy metabolism in brown adipocytes.
Conclusion: *Nat8l* expression influences cellular bioenergetics in adipocytes.
Significance: These findings establish a novel pathway in brown adipocyte metabolism.

NAT8L (*N*-acetyltransferase 8-like) catalyzes the formation of *N*-acetylaspartate (NAA) from acetyl-CoA and aspartate. In the brain, NAA delivers the acetate moiety for synthesis of acetyl-CoA that is further used for fatty acid generation. However, its function in other tissues remained elusive. Here, we show for the first time that *Nat8l* is highly expressed in adipose tissues and murine and human adipogenic cell lines and is localized in the mitochondria of brown adipocytes. Stable overexpression of *Nat8l* in immortalized brown adipogenic cells strongly increases glucose incorporation into neutral lipids, accompanied by increased lipolysis, indicating an accelerated lipid turnover. Additionally, mitochondrial mass and number as well as oxygen consumption are elevated upon *Nat8l* overexpression. Concordantly, expression levels of brown marker genes, such as *Prdm16*, *Cidea*, *Pgc1α*, *Pparα*, and particularly UCP1, are markedly elevated in these cells. Treatment with a PPARα antagonist indicates that the increase in UCP1 expression and oxygen consumption is PPARα-dependent. *Nat8l* knockdown in brown adipocytes has no impact on cellular triglyceride content, lipogenesis, or oxygen consumption, but lipolysis and brown marker gene expression are increased; the latter is also observed in BAT of *Nat8l*-KO mice. Interestingly, the expression of ATP-citrate lyase is increased in *Nat8l*-silenced adipocytes and BAT of *Nat8l*-KO mice, indicating a compensatory mechanism to sustain the acetyl-CoA pool once *Nat8l* levels are reduced. Taken together, our data show that *Nat8l* impacts on the brown adipogenic phenotype and suggests the existence of the NAT8L-driven NAA metabolism as a novel pathway to provide cytosolic acetyl-CoA for lipid synthesis in adipocytes.

Adipose tissue depots are critical organs for the control of energy homeostasis. White adipose tissue (WAT) is the major fat-storing organ in the body, and its adipocytes are characterized by large, unilocular lipid droplets and only few mitochondria. During energy demand, triglycerides (TG)[3] are broken down to supply peripheral tissues with fatty acids (1, 2). Brown adipocytes are characterized by multiple, smaller lipid droplets and numerous mitochondria, which contain UCP1, a protein that uncouples oxidative phosphorylation from ATP production to dissipate energy into heat (3). With the discovery of active brown adipose tissue (BAT) in adult humans (4–7) and its association with leanness (5), much attention has been paid to the investigation of BAT development and homeostasis due to its possible role in fighting obesity and its associated disorders (8). Recently, it has been shown that adipose triglyceride lipase-mediated breakdown of TG is required for a distinct brown adipose phenotype in mice (9). Thus, it seems that a

* This work was supported by Austrian Science Fund FWF Grants DK-MCD W01226 and P24143, by Program for Next Generation World-leading Researchers Grant LS047, and by a Smoking Research Foundation Grant for Biomedical Research.
[1] Both authors contributed equally to this work.
[2] To whom correspondence should be addressed: Petersgasse 14/5, 8010 Graz, Austria. Tel.: 43-316-873-5337; E-mail: juliane.bogner-strauss@tugraz.at.

[3] The abbreviations used are: TG, triglyceride(s); WAT, white adipose tissue; BAT, brown adipose tissue; FFA, free fatty acids; PPAR, peroxisome proliferator-activated receptor; NAA, *N*-acetylaspartate; iBACs, immortalized brown adipogenic cells; ER, endoplasmic reticulum; BisTris, 2-[bis(2-hydroxyethyl)amino]-2-(hydroxymethyl)propane-1,3-diol; OCR, oxygen consumption rate.

large proportion of fatty acid has first to be stored as TG and thereafter hydrolyzed before they can be used for UCP1 activation (and mitochondrial β-oxidation). Additionally, activated BAT shows high rates of glucose uptake (10), but glucose is suggested to play only a minor role as a direct oxidative substrate (11). Therefore, enzymes involved in *de novo* lipid synthesis are highly expressed in BAT and further increased upon thermogenic activation (12).

Many of the identified molecular network components controlling white and brown metabolism have been disclosed by the use of novel high throughput technologies. Among others, we performed microarray studies in white and brown adipose tissue of *Atg*- and *Hsl*-KO mice (13) and focused on candidate genes that might be of interest in the development and metabolism of adipose tissues. Among these was a gene encoding for the enzyme NAT8L (*N*-acetyltransferase 8-like).

In the brain, NAT8L was shown to catalyze the formation of *N*-acetylaspartate (NAA) from acetyl-CoA and L-aspartate (14, 15). NAA then acts as a carrier of acetyl groups between neurons and oligodendrocytes where NAA is catabolized by aspartoacylase into acetate and L-aspartate (16). The acetate moiety is reutilized for acetyl-CoA synthesis and can subsequently be incorporated into lipids (16, 17). The metabolic importance of NAA has been shown in two inborn human neurodegenerative disorders, where defects in NAA biosynthesis (14, 18) as well as catabolism (19) lead to reduced myelin synthesis.

Here, we describe for the first time that *Nat8l* is highly expressed in adipocytes and that its expression is induced during the differentiation of various mouse and human adipogenic cells. Furthermore, overexpression of *Nat8l* in an immortalized brown adipogenic cell line influenced lipid turnover, increased mitochondrial mass, and accelerated energy expenditure, most likely by increasing the expression of UCP1 in a PPARα-dependent manner. Our results from *Nat8l* silencing in brown adipocytes and from examining BAT in *Nat8l*-KO mice support the hypothesis that the NAT8L/NAA pathway acts as an alternative source to provide acetyl-CoA as a building block for lipid biosynthesis in adipocytes. These data suggest that the NAA pathway exists and is functional in adipose tissue and that modulating this pathway could be a valuable new approach to increase energy dissipation in (brown) adipocytes.

EXPERIMENTAL PROCEDURES

Cell Culture, Differentiation, Lipid Staining, and Quantification—Immortalized brown adipogenic cells (iBACs) were grown in DMEM containing 10% FBS, 50 μg/ml streptomycin, 50 units/ml penicillin, and 20 mM Hepes. C3H-10T1/2 cells were grown and maintained in DMEM containing 10% FBS and penicillin/streptomycin. C3H-10T1/2 cells were induced to differentiate 2 days after confluence with 0.5 mM 3-isobutyl-1-methylxanthine, 1 μM dexamethasone, 2 μg/ml insulin, and 1 μM rosiglitazone (Cayman Chemical). After 3 days, medium was changed to maintenance medium with 2 μg/ml insulin and 1 μM rosiglitazone, and 48 h thereafter, normal growth medium was used until harvest. Simpson-Golabi-Behmel syndrome cells were cultured and differentiated as described by us elsewhere (20). iBACs were induced to differentiate at the day of confluence with 0.5 mM 3-isobutyl-1-methylxanthine, 0.5 μM dexamethasone, 20 nM insulin, 1 nM triiodthyronine, and 125 μM indomethacin. Two days after induction, medium was changed to maintenance medium containing 20 nM insulin and 1 nM triiodthyronine, and cells were kept in this medium until harvest. Cells were fixed (10% formalin in PBS for 30 min), rinsed in PBS, and stained with oil red O (0.25% in 60% isopropyl alcohol stock solution diluted 3:2 with distilled H_2O for 30 min). To stimulate thermogenesis, cells were incubated with 1 μM isoproterenol for 4 h. iBACs were treated with 10 μM PPARα antagonist GW6471 (Tocris Bioscience) from day 4 until harvest. Cellular triglyceride content was determined in differentiated iBACs using Infinity Triglyceride Reagent (Thermo). Free fatty acid content was measured using the NEFA C test kit (WAKO). Values were corrected by protein content measurement using BCA reagent (Pierce).

Animal Studies—Male C57BL/6 and ob/ob mice at the age of 24–26 weeks were used for this study. Before harvesting tissue pads, mice were fasted for 12 h, following refeeding for 1 h. *Nat8l*-knock-out mice (21) and their controls were used at the age of 3–4 months and fed *ad libitum* before harvesting tissues. Animals were kept on a 12-h light/dark cycle on a normal chow diet. All animal procedures followed the National Institutes of Health Guidelines for the Care and Use of Laboratory Animals and were approved by the Austrian Ministry for Science and Research and the Committee for Animal Experiments of the University of Toyama.

Retroviral Expression of Nat8l in Monoclonal Cell Lines—Full-length coding sequence of murine *Nat8l* was amplified by PCR from murine adipose tissue cDNA using *Phusion* polymerase (Fermentas) and cloned into a murine stem cell virus vector (pMSCV puro, BD Biosciences Clontech) using the restriction sites XhoI/EcoRI. To produce infectious but replication-incompetent recombinant retroviruses expressing *Nat8l*, PhoenixEco packaging cells (cultured in DMEM with 10% FBS in 5% CO_2) were transfected with pMSCV-*Nat8l* using Metafectene (Biontex Laboratories GmbH). The supernatant containing the viral particles was collected 48 h after transfection. Viral supernatants were supplemented with 8 μg/ml Polybrene and added to iBACs (30–40% confluence) for infections for 18–24 h. Because cells could not be selected with puromycin, single cells were picked under the microscope and expanded as monoclonal populations, and overexpression was controlled by quantitative RT-PCR. Differentiation was induced as described above. As a control for the above described stable cell lines, the empty pMSCVpuro was used and underwent the same procedure.

Silencing of Nat8l Using Short Hairpin RNA (shRNA)-containing Lentiviral Particles—One control non-targeting shRNA lentivirus and two shRNA lentiviruses directed against *Nat8l* were purchased from Sigma (MISSION™ shRNA lentiviral particles NM_001001985). iBACs were seeded into 6-well plates 12 h before transduction using 3×10^4 cells/well (around 30% confluence). Cells were infected for 16 h with a multiplicity of infection of 10 in complete medium containing 8 μg/ml Polybrene (Sigma). After transduction, the infection medium was replaced with fresh medium, and the cells underwent the same selection process as *Nat8l*-overexpressing iBACs.

TABLE 1
Primer pairs used for quantitative RT-PCR
All primers were used with murine cDNA except for the indicated human primers.

Target gene	Forward primer (5′ → 3′)	Reverse primer (5′ → 3′)
Human *NAT8L*	TGTGCATCCGCGAGTTCCGT	CGGAAGGCCGTGTTAGGGAT
Human *β-ACTIN*	CGCCGCATCCTCCTCTTC	GACACCGGAACCGCTCATT
Murine *Nat8l*	TGTGCATCCGCGAGTTCCGC	GCGGAAAGCCGTGTTGGGGA
Tfiiβ	GTCACATGTCCGAATCATCCA	TCAATAACTCGGTCCCCTACAA
Pparγ2	TGCCTATGAGCACTTCACAAGAAAT	CGAAGTTGGTGGGCCAGAA
Fabp4/aP2	CGACAGGAAGGTGAAGAGCATC	ACCACCAGCTTGTCACCATCTC
Adipoq	TGTTCCTCTTAATCCTGCCCA	CCAACCTGCACAAGTTCCCTT
Fads3	GTGATCCACACGAACCAGTG	TCCCGCTTTTTCTTGTCCTAC
Retn	AAGAAGGAGCTGTGGGACAGG	CAGCAGTTCAGGGACAAGGAA
Psat1	AGTGGAGCGCCAGAATAGAA	TACCGCCTTGTCAAGAAACC
Pgc1α	TCTCTGGAACTGCAGGCCTAAC	TCAGCTTTGGCGAAGCCTT
Pparα	CCTGAACATCGAGTGTCGAATATG	GCGAATTGCATTGTGTGACATC
Prdm16	TCCACAGCACGGTGAAGCCA	ATCTGCGTCCTGCAGTCGGC
C/ebpβ	GGACTTGATGCAATCCGGA	AACCCCGCAGGAACATCTTTA
Cox8b	GCGAAGTTCACAGTGGTTCC	AACCATGAAGCCAACGACTATG
Cidea	TGACATTCATGGGATTGCAGAC	GGCCAGTTGTGATGACTAAGAC
Ucp1	ACACCTGCCTCTCTCGGAAA	TAGGCTGCCCAATGAACACT
Dio2	AACAGCTTCCTCCTAGATGCC	CATCAGCGGTCTTCTCCGAG
Cox1	TGAGCCCACCACATATTCACAG	AGGGTTGCAAGTCAGCTAAATAC
Cpt1b	TGTATCGCCGCAAACTGGACCG	TCTGGTAGGAGCACATGGGCAC
Pdk4	TTTCTCGTCTCTACGCCAAG	GATACACCAGTCATCAGCTTCG
Fabp3	CCTTTGTCGGTACCTGGAAGCT	AAAGCCCACACCGAGTGACTT
Acly	AGGAAGTGCCACCTCCAACAGT	CGCTCATCACAGATGCTGGTCA

Site-directed Mutagenesis of Nat8l and Subsequent Stable Transfection of iBACs—For better selectivity, *Nat8l* coding sequence was transferred into a pMSCV-hygro vector (kind gift from E. D. Rosen). Site-directed mutagenesis was performed by PCR amplification with *Phusion* polymerase using pMSCV-*Nat8l* as template with the following primers (base substitution is marked as a lowercase letter): *Nat8l*_D165A_fw, 5′-TGCACACGGCcATGGCTGACATTGAGCAGTACTACATGAAGC-3′; *Nat8l*_D165A_rv, 5′-AGCCATgGCCGTGTGCAGCGCACACTCCAGGTAGGC-3′. This led to a subsequent change from aspartic acid to alanine. The purified PCR product was digested for 1 h at 37 °C with 20 units of DpnI in order to eliminate the template, and the mutated vector was transformed into *Escherichia coli*. The complete *Nat8l* coding region was sequenced to verify the presence of the introduced mutation and the absence of random mutations. iBACs overexpressing *Nat8l*_D165A were generated as described above with pMSCV-hygro as a control. Selection of positive clones was performed with 500 μg/ml hygromycin for at least 7 days.

Mitochondria Isolation and Western Blot Analysis—Mitochondria were isolated from cell pellets of differentiated iBACs with a commercially available kit (Thermo Scientific) using the Dounce homogenizer and 3000 × *g* to pellet the mitochondria. BAT mitochondria were isolated as described previously (22). Modifications to the protocol were as follows. The tissues were excised from male mice fed *ad libitium*, washed in ice-cold PBS, and cut into small pieces with a razorblade. Subsequently, they were homogenized using a Dounce homogenizer with about 60 strokes. The centrifugation steps to pellet the mitochondria were carried out at 3000 × *g* to reduce peroxisomal contamination. Nuclear fraction, mitochondrial fraction, and post-mitochondrial supernatant containing cytosol and ER remnants were lysed in SDS-lysis buffer (50 mM Tris-HCl, pH 6.8, 10% glycerol, 2.5% SDS, 1× protease inhibitor mixture, 1 mM PMSF) and used for further analysis. Cytosolic/ER proteins have been precipitated using the trichloroacetic acid (TCA) method. Briefly, cytolytic protein lysate was mixed with 50% ice-cold TCA to obtain a concentration of 10% TCA and incubated for 1.5 h on ice. Then it was centrifuged for 10 min at 13,000 rpm and 4 °C. The pellet was washed twice with ice-cold acetone, air-dried, and dissolved in SDS-lysis buffer. Control and *Nat8l*-overexpressing iBACs (at several differentiation time points) were harvested for protein analysis by scraping with SDS-lysis buffer. After benzonase digestion, protein concentrations were determined with the BCA protein assay kit (Pierce). 50 μg of sample were subjected to a 12% BisTris gel (NuPAGE, Invitrogen), and gels were blotted to nitrocellulose membranes. The following antibodies were used: anti-NAT8L (1:1000) (Novus Biologicals, catalog no. NBP1-06599); anti-UCP1 (1:1000) (Calbiochem); anti-hexokinase (1:1000), anti-histone H3 (1:2000), and anti-protein-disulfide isomerase (1:1000) (all from Cell Signaling Technology); and anti-β-Actin (1:25,000) (Sigma). For chemiluminescent detection, a horseradish peroxidase-conjugated secondary antibody was used (anti-rabbit; 1:5000) (DAKO), and ECL (Pierce) served as substrate.

RNA Isolation, Reverse Transcription, and Gene Expression Analysis—Total RNA from cells was isolated using the Total RNA isolation kit (Sigma). Tissue RNA was isolated with TRIzol reagent (Invitrogen). cDNA was generated using Superscript II reverse transcriptase (Invitrogen). mRNA expression was assessed using real-time PCR as described (20). Gene expression was normalized to *Tfiiβ* in murine tissues and cells and to *β-ACTIN* in human cells. For a primer list, see Table 1.

Measurement of Cellular Oxygen Consumption Rate (OCR)—Six days after inducing differentiation, iBACs were plated in XF96 polystyrene cell culture microplates (Seahorse Bioscience) at a density of 40,000 cells/well. After an overnight incubation, cells were washed and preincubated for 30 min in unbuffered XF assay medium (Seahorse Bioscience) supplemented with 5.5 mM D-glucose and 1 mM sodium pyruvate at 37 °C in a non-CO_2 environment. OCR was subsequently measured every 7 min using an XF96 extracellular flux analyzer (Seahorse Bioscience). Optimal concentrations of specific inhibitors/accelerators of the electron transport chain were

determined in prior titration experiments, and working concentrations used were 1 μM oligomycin, 2 μM carbonyl cyanide *p*-trifluoromethoxyphenylhydrazone, 2.5 μM antimycin A, and 10 μM norepinephrine.

[^{14}C]Glucose Uptake and Lipid Extraction—iBACs were incubated overnight with DMEM supplemented with 1 nM triiodthyronine, 20 nM insulin, 0.5 g/liter glucose, and 0.1 μCi of D-[^{14}C(U)]glucose/ml (ARC). After that, cells were washed four times with ice-cold PBS, and neutral lipids were extracted with hexane/isopropyl alcohol (3:2, v/v). Thin layer chromatography was performed with hexane/diethylether/acetic acid (70/29/1, v/v/v) as solvent, and lipids were visualized with iodine vapor and cut out. The incorporated radioactivity was measured by liquid scintillation counting. Total glucose incorporation in each lipid class was calculated, and values were corrected by protein content.

Detection of Mitochondrial Mass by Flow Cytometry—iBACs were grown until day 7 of differentiation, trypsinized, incubated for 20 min in DMEM supplemented with 200 nM MitoTracker™ Green (Invitrogen), washed with PBS, and subjected directly to flow cytometry (BD FACSCalibur, BD Biosciences). 90% of all cells were found in sectors II and IV. Sector II was chosen to compare fluorescence intensities between control and *Nat8l*-overexpressing cells.

Transmission Electron Microscopy—Transmission electron microscopy was performed as described (23). In brief, iBACs grown on an Aclar film (Gröpl, Tulln, Austria) were fixed on day 7 in 2.5% (w/v) glutaraldehyde and 2% (w/v) paraformaldehyde in 0.1 M phosphate buffer, pH 7.4, for 1 h, postfixed in 2% (w/v) osmium tetroxide for 1 h at room temperature, dehydrated in a graded series of ethanol, and embedded in a TAAB epoxy resin (Gröpl). Ultrathin sections (75 nm) were cut with a Leica UC 6 Ultramicrotome and stained with lead citrate for 5 min and with uranyl acetate for 15 min. Images were taken using a FEI Tecnai G2 20 transmission electron microscope (FEI Eindhoven) with a Gatan ultrascan 1000 CCD camera. The acceleration voltage was 120 kV.

Measurement of Mitochondrial Membrane Potential—iBACs were plated on 30-mm glass coverslips on day 7. Following overnight incubation, cells were loaded with a 500 nM concentration of the ratiometric indicator JC-1 (Invitrogen) in full medium at 37 °C for 30 min. Cells were then washed, and fluorescence intensities were detected over mitochondrial regions using an array confocal laser-scanning microscope built on an inverse, automatic microscope (Axio Observer.Z1, Zeiss, Germany) equipped with a ×100, 1.45 numerical aperture oil immersion objective (Plan-Fluor, Zeiss), an acousto-optic tunable filter-based laser merge system (Visitron Systems), and a CCD camera (CoolSNAP-HQ, Photometrics). Excitation/emission wavelengths were 488/529 and 535/590 nm for green fluorescent monomers and red fluorescent J-aggregates, respectively. During experiments, cells were perfused with a buffer containing 145 mM NaCl, 5 mM KCl, 2 mM $CaCl_2$, 1 mM $MgCl_2$, 10 mM D-glucose, and 10 mM HEPES, pH 7.4. Basal fluorescence intensity ratios were normalized to corresponding ratios after dissipation of mitochondrial membrane potential using 2 μM carbonyl cyanide *p*-trifluoromethoxyphenylhydrazone.

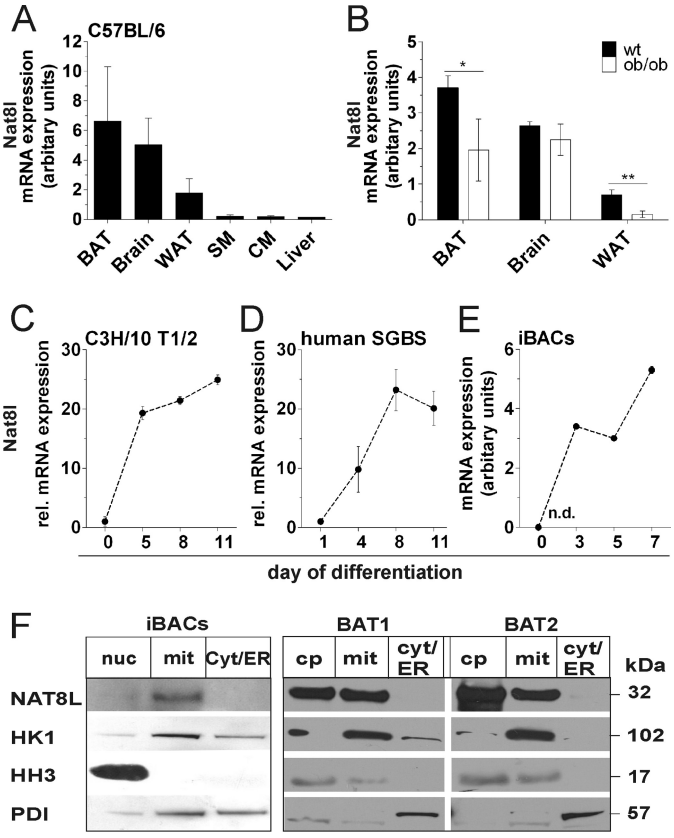

FIGURE 1. ***Nat8l* is expressed in adipocytes, is strongly decreased in WAT and BAT of genetically obese mice, and localizes in mitochondria *in vitro* and *in vivo*.** *A* and *B*, quantitative real-time PCR analysis of *Nat8l* mRNA expression in various tissues of male, refed C57BL/6 mice (*A*), and ob/ob mice (*B*) ($n = 4$). *BAT*, brown adipose tissue; *WAT*, white adipose tissue; *SM*, skeletal muscle; *CM*, cardiac muscle. *C–E*, *Nat8l* mRNA in various adipogenic cell lines during differentiation ($n \geq 3$). *C* and *D*, expression at the start of differentiation is set to 1. *C*, murine, mesenchymal white adipogenic cells C3H/10 T1/2. *D*, human, white adipogenic Simpson-Golabi-Behmel syndrome (*SGBS*) cells. *E*, murine iBACs. All data are presented as means ± S.D. (*error bars*). *F*, protein expression of NAT8L in iBACs and C57BL/6 BAT fractionates (*cp*, crude pellet; *mit*, mitochondria; *nuc*, nucleus; *cyt/ER*, cytosol/endoplasmic reticulum). Shown is one representative blot of $n = 3$ (*left*) and $n = 2$ (*right*). *, $p < 0.05$; **, $p < 0.01$.

Statistical Analysis—If not otherwise stated, results are mean values ± S.D. of at least three independent experiments, or results show one representative experiment of three. Statistical analysis was done on all available data. Statistical significance was determined using the two-tailed Student's *t* test. *, $p < 0.05$; **, $p < 0.01$; ***, $p < 0.001$.

RESULTS

Nat8l Is Expressed in Adipocytes and Located in Mitochondria—NAT8L is often referred to as a brain-specific enzyme, and it is still under debate whether it is located in the mitochondria or ER/cytoplasm of neurons (24–26). Fig. 1*A* shows that *Nat8l* is expressed to a similar extent in brain and BAT, to a lower extent in WAT, and hardly detectable in skeletal muscle (*SM*), cardiac muscle (*CM*), and liver of C57BL/6 mice. In genetically obese mice (ob/ob), the *Nat8l* mRNA level was unchanged in the brain, whereas it was 50% decreased in BAT and nearly blunted in WAT when compared with WT mice (Fig. 1*B*). We next determined the expression profile of *Nat8l* during the differentiation of several adipogenic cell lines.

Nat8l mRNA expression increases about 20-fold during white adipogenic differentiation of C3H10 T1/2 cells (Fig. 1*C*). A similar increase was observed in human Simpson-Golabi-Behmel syndrome adipogenic cells (Fig. 1*D*). Most relevant for this work, *Nat8l* mRNA levels highly increased during differentiation of iBACs (Fig. 1*E*). Next, we investigated the localization of endogenous NAT8L in differentiating iBACs and BAT by subjecting subcellular fractionations to Western blot analysis. NAT8L protein could be clearly detected in the mitochondrial fraction, both *in vitro* (Fig. 1*F*, *left panel*) and *in vivo* (Fig. 1*F*, *right panels*), and there was no detectable NAT8L protein in the ER/cytosolic fraction. To control proper fractionation, we included hexokinase 1 (mitochondrial), histone H3 (nuclear), and protein disulfide isomerase (cytosolic) detection. Due to its high expression in BAT, we focused on iBACs as a model system to study the role of *Nat8l* in adipocyte biology.

Overexpression of Nat8l in Differentiating iBACs Increases Lipid Turnover—In brain, NAT8L has been shown to be required for lipid synthesis, especially for myelination (14, 16). To analyze the influence of *Nat8l* on lipid metabolism in brown fat cells, we generated iBACs stably overexpressing *Nat8l*. After clonal expansion, cells were induced to differentiate into brown adipocytes. Two monoclonal populations exhibited substantial overexpression of *Nat8l* (-fold expression relative to control on day 3 of differentiation: 28.9 ± 8.4 and 12.3 ± 0.5, respectively). To measure neutral lipid synthesis from glucose, iBACs were incubated with ^{14}C-labeled glucose. *Nat8l*-overexpressing iBACs showed an up to 4-fold increased incorporation of glucose into neutral lipids, such as diglycerides, TG, FFA, and cholesteryl ester, on day 3 (Fig. 2*A*) and day 7 of differentiation (Fig. 2*B*). However, oil red O staining and TG measurements of *Nat8l*-overexpressing and control iBACs showed decreased TG levels on day 3 (Fig. 2*C*; quantified in Fig. 2*D*), whereas even a slight increase in lipid accumulation could be observed on day 7 of differentiation (Fig. 2*C*; quantified in Fig. 2*E*). The fact that, despite higher glucose incorporation into neutral lipids, TG accumulation was delayed in differentiating *Nat8l*-overexpressing iBACs prompted us to investigate lipolysis. Therefore, we measured glycerol and FFA content in cell lysates and supernatants of *Nat8l*-overexpressing and control iBACs on day 7. Whereas glycerol release (Fig. 2*E*) showed a tendency to decrease, FFA release was increased 4-fold in differentiated *Nat8l*-overexpressing iBACs compared with control cells (Fig. 2*F*). Additionally, we observed a 3-fold increase in FFA release upon isoproterenol stimulation in *Nat8l*-overexpressing cells (Fig. 2*F*). However, FFA content in cell lysates was not changed in any condition (Fig. 2*F*). Collectively, our data suggest an increased lipid turnover upon *Nat8l* overexpression in brown adipocytes.

Nat8l Overexpression Increases Mitochondrial Mass, Number, and Cellular Respiration Rate—Because lipolysis is a requirement for a distinct brown adipose phenotype *in vivo* (9), we asked whether mitochondrial mass, number, and cellular respiration rates are changed in *Nat8l*-overexpressing iBACs. Transmission electron microscopy clearly demonstrates an increased number of mitochondria in *Nat8l*-overexpressing cells (Fig. 3*A*). Counting 14 individual cells from two biological replicates from either control or *Nat8l*-overexpressing iBACs

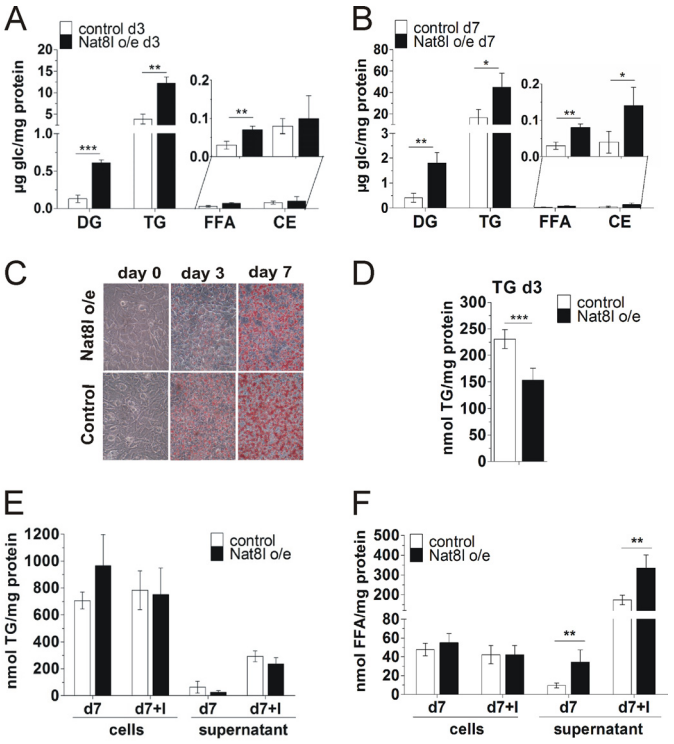

FIGURE 2. **Overexpression of *Nat8l* increases lipid turnover in iBACs.** iBACs were infected with retroviral particles harboring either *Nat8l* coding sequence or empty vector as control. *A*, incorporation of [^{14}C]glucose into neutral lipids of day 3 iBACs. iBACs were incubated with D-[^{14}C(U)]glucose overnight, neutral lipids were extracted and separated by TLC, and incorporated radioactivity was counted and calculated as glucose uptake ($n = 3$). *B*, incorporation of [^{14}C]glucose into neutral lipids of day 7 iBACs. *C*, oil red O stainings of *Nat8l*-overexpressing (*o/e*) and control iBACs during differentiation. Representative micrographs of $n = 3$ are shown. *D*, triglyceride quantification of cell lysates of *Nat8l*-overexpressing and control iBACs on day 3 of differentiation ($n = 3$). *E*, TG content in control and *Nat8l*-overexpressing cell lysates and supernatants in basal conditions and after isoproterenol stimulation (10 μM for 4 h; *+I*) ($n = 3$). *F*, fatty acid content in cell lysates and supernatants of *Nat8l*-overexpressing and control cells with and without isoproterenol treatment (10 μM for 4 h; *+I*) ($n = 3$). All data are presented as means ± S.D. (*error bars*), two-tailed Student's *t* test. *, $p < 0.05$; **, $p < 0.01$; ***, $p < 0.001$.

revealed a doubling of mitochondria/cell upon *Nat8l* overexpression (Fig. 3*B*). Furthermore, we incubated cells with MitoTracker Green, which stains mitochondria in a membrane potential-independent manner (27) and subjected them to flow cytometry. As depicted in Fig. 3, *C* (*sector II*) and *D*, *Nat8l*-overexpressing cells showed increased fluorescence intensity, indicating an increased mitochondrial mass. Nevertheless, others reported that MitoTracker Green changes its abilities with regard to the membrane potential (28). To ascertain that the increase in fluorescence intensity was not due to a membrane potential change, we measured membrane potential via incubation with the mitochondrial stain JC-1. As shown in Fig. 3*E*, there was no significant change in membrane potential in *Nat8l*-overexpressing cells when compared with controls. The increased mitochondrial mass led us to hypothesize that *Nat8l*-overexpressing cells may have an elevated OCR. Therefore, we studied the cells with a Seahorse extracellular flux analyzer. This experiment revealed that *Nat8l*-overexpressing cells have an increased OCR (Fig. 3*F*). Specifically, basal respiration and maximal respiration were elevated by at least 40%. Even in an activated state, after preincubation with 10 μM norepinephrine for

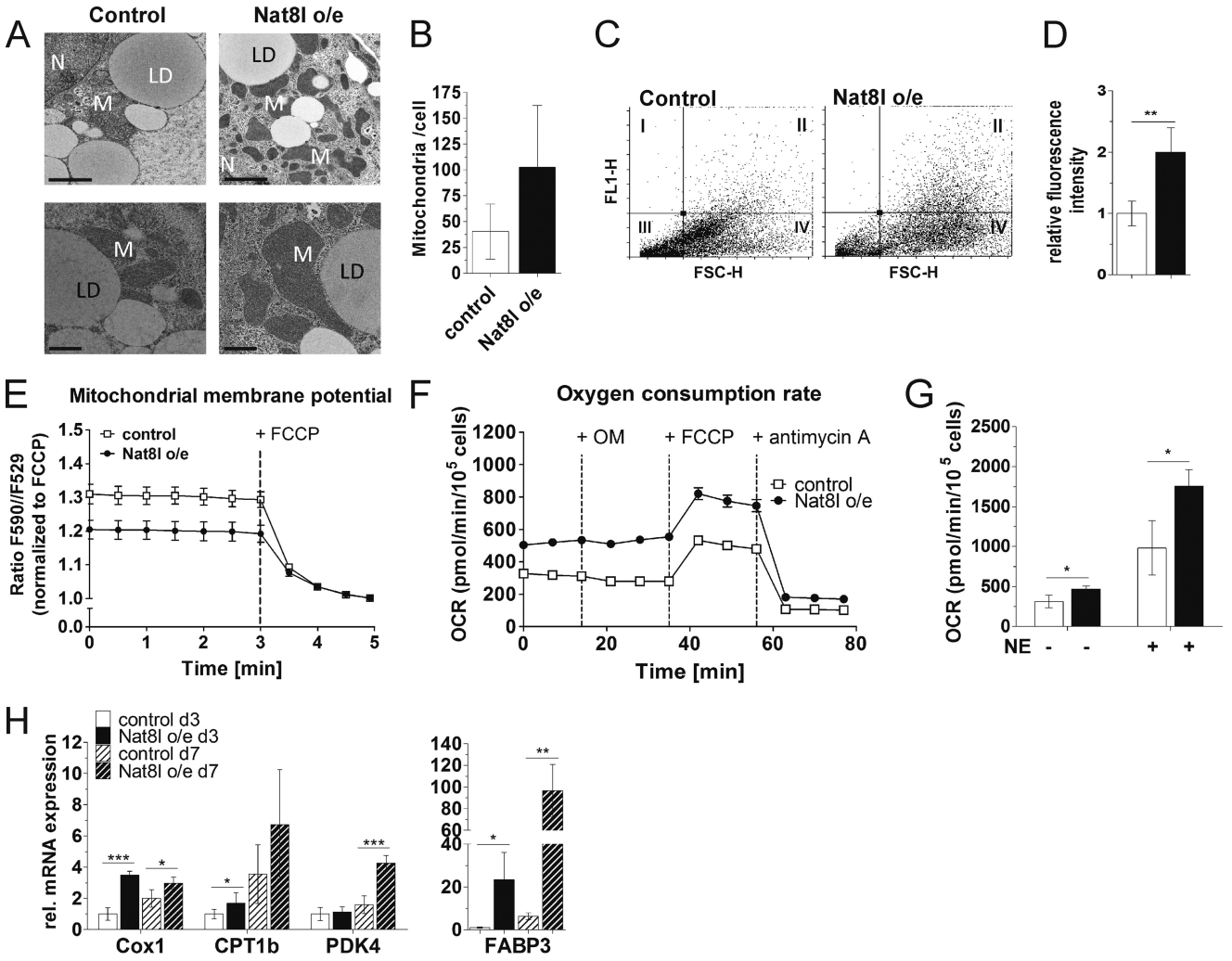

FIGURE 3. ***Nat8l* overexpression increases mitochondrial mass and energy expenditure in iBACs.** *A*, transmission electron micrograph of *Nat8l*-overexpressing and control iBACs on day 7. *Scale bars*, 2 μm (*top panels*) and 1 μm (*bottom panels*); *LD*, lipid droplet; *M*, mitochondria; *N*, nucleus. *B*, mitochondria count of 14 individual cells from control and *Nat8l*-overexpressing cells. *C*, iBACs were incubated with 200 nM MitoTracker Green and subjected to flow cytometry. Fluorescence intensity was measured in FL-1. FSC-H is a measure for cell size ($n = 3$). *D*, quantification of fluorescence intensity in sector II shows the relative increase in mitochondrial mass ($n = 3$). *E*, mitochondrial membrane potential was measured using JC1 as a mitochondrial stain. JC1 fluorescence shifts from 529 nm (*green*) to 590 nm (*red*) upon a drop in membrane potential. The ratio from 590/529 nm was measured to estimate the relative membrane potential before and after carbonyl cyanide *p*-trifluoromethoxyphenylhydrazone (*FCCP*) treatment. Data are shown as means ± S.E. (*error bars*), $n = 2$. *F*, OCR of iBACs on day 7 measured with the Seahorse extracellular flux analyzer. Cells were treated at the indicated time points with 1 μM oligomycin (*OM*), 2 μM carbonyl cyanide *p*-trifluoromethoxyphenylhydrazone, and 2.5 μM antimycin A. Data shown as means ± S.E. (*error bars*) ($n = 3$). *G*, OCR of iBACs after a 1-h preincubation with 10 μM norepinephrine (*NE*) ($n = 3$). *H*, mRNA expression of genes involved in mitochondrial oxidative phosphorylation (*Cox1*) and β-oxidation (*Cpt1b*, *Pdk4*, and *Fabp3*) was measured in day 3 and day 7 iBACs ($n = 3$). If not otherwise stated, data are presented as means ± S.D. (*error bars*), two-tailed Student's *t* test. *, $p < 0.05$; **, $p < 0.01$; ***, $p < 0.001$.

1 h, increased respiration was evident in *Nat8l*-overexpressing cells compared with control cells (Fig. 3*G*). In addition, genes that are directly involved in mitochondrial oxidative phosphorylation (*Cox1*, mitochondrial coded subunit of *Cytc*) and indirectly in β-oxidation (*Cpt1b* (carnitine palmitoyltransferase 1b), *Pdk4* (pyruvate dehydrogenase kinase 4), and *Fabp3* (fatty acid-binding protein 3)) were significantly up-regulated on day 3 and/or day 7 of differentiation of *Nat8l*-overexpressing cells, respectively (Fig. 3*H*). In summary, these data indicate increased energy expenditure in iBACs upon *Nat8l* overexpression.

Nat8l Overexpression Augments the Brown Adipose Phenotype—Although TG accumulation is significantly decreased in *Nat8l*-overexpressing iBACs on day 3, no significant changes in expression profiles of general adipogenic markers, such as aP2 and adiponectin (*AdipoQ*), could be observed (Fig. 4*A*). As an exception, *Pparγ2* levels were 3-fold increased on day 3 but reached the level of control cells by day 7. Additionally, three white selective markers (29) were investigated. Whereas the expression of fatty acid desaturase 3 (*Fads3*) did not change, phosphoserine aminotransferase 1 (*Psat1*) and resistin (*Retn*) were significantly decreased in *Nat8l*-overexpressing cells (Fig. 4*A*). Notably, the expression of genes that are crucial in the development of brown adipocytes, such as *Pparα*, *Pgc1α* (*Pparγ* coactivator 1 α), *Prdm16*, *C/ebpβ*, *Cox8b*, *Dio2*, and *Cidea*, were all increased in *Nat8l*-overexpressing iBACs on day 7 (Fig. 4*B*). Strikingly, *Ucp1* mRNA expression was increased up to 17-fold in *Nat8l*-overexpressing iBACs on day 7 (Fig. 4*C*), and its expression could be further elevated upon the addition of 10 μM isoproterenol (Fig. 4*C*), showing that *Nat8l*-overexpressing cells still have the potential to be activated by β-adrenergic stim-

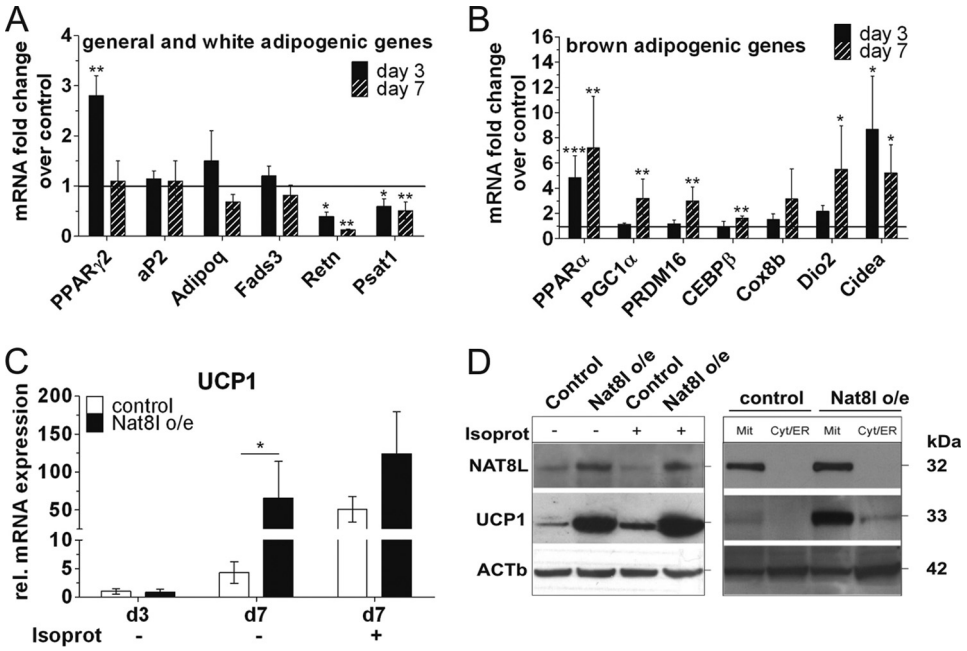

FIGURE 4. ***Nat8l* overexpression augments the brown adipose phenotype.** *A*, mRNA expression of general (*Pparγ2*, *aP2*, and *Adipoq*) and white adipogenic genes (*Fads3*, *Psat1*, and *Retn*) in day 3 and day 7 iBACs ($n \geq 3$). *B*, mRNA expression of brown marker genes in day 3 and day 7 iBACs ($n \geq 3$). Data in *A* and *B* are expressed as -fold change of Nat8l-overexpressing *versus* control iBACs. Shown is *Ucp1* mRNA (*C*) and UCP1 and NAT8L protein expression (*D*, *left*) with and without 10 μM isoproterenol stimulation for 4 h on day 7 in control and *Nat8l*-overexpressing iBACs. *D* (*right*), protein expression of NAT8L in fractionated iBACs. UCP1 served as a mitochondrial marker. *Mit*, mitochondria; *Cyt/ER*, cytosol/ER. β-ACTIN (*ACTb*) served as a loading control. One representative blot of $n = 3$ is shown. All data are presented as means ± S.D. (*error bars*), two-tailed Student's *t* test. *, $p < 0.05$; **, $p < 0.01$; ***, $p < 0.001$.

ulation. This enormous induction of UCP1 upon *Nat8l* overexpression could also be confirmed at the protein level (Fig. 4*D*, *left*). To test whether overexpressed NAT8L protein is located in mitochondria like the endogenous one (Fig. 1*E*), a fractionation of *Nat8l*-overexpressing iBACs was performed on day 7. NAT8L localized exclusively in the mitochondria, as did UCP1, a described mitochondrial protein (Fig. 4*D*, *right*). Hence, we observe an increased brown phenotype upon *Nat8l* overexpression.

Nat8l Overexpression Increases UCP1 Levels and OCR in a PPARα-dependent Manner—PPARα was shown to increase expression of *Ucp1*, the protein mainly responsible for a brown phenotype. Furthermore, the activation potential of PPARα is enhanced by lipolytic products (30). We observed both increased lipolysis (Fig. 2*F*) and enhanced expression of *Ucp1* in *Nat8l*-overexpressing iBACs (Fig. 4*C*). Hence, we reasoned that these changes are mediated by PPARα. Therefore, we treated *Nat8l*-overexpressing iBACs with a PPARα antagonist (10 μM GW6471) from day 4 of differentiation until day 7. This treatment did not change differentiation capacity as judged by microscopy and cellular TG content (Fig. 5*E*). Measuring mRNA levels of marker genes upon PPARα antagonist treatment, we found that *Pgc1α* and *aP2* were unchanged, and *Cox1* and *Pdk4* were slightly decreased, whereas the direct PPARα target genes *Cpt1b* (31) and *Ucp1* (32) were significantly blunted (Fig. 5*A*). Importantly, the massive *Nat8l*-mediated up-regulation in UCP1 protein was nearly reduced to control level (Fig. 5*B*). In accordance, OCR was reduced close to the level of control cells after GW6471 treatment of Nat8l-overexpressing cells (Fig. 5*C*). On the other hand, neither the increased lipogenesis (Fig. 5*D*) nor the elevated basal and isoproterenol-stimulated FFA release evoked by *Nat8l* overexpression was affected by GW6471 treatment (Fig. 5*F*). These results underline our hypothesis that *Nat8l per se* influences lipid turnover, but other effects, such as UCP1 and *Cpt1b* expression and respiration, require PPARα activation.

Enzymatic Activity Is Required for the Function of NAT8L in Adipocytes—Recently, Tahay *et al.* (24) investigated which regions of the human NAT8L protein are important for its catalytic activity by introducing several point mutations into the *Nat8l* gene and subsequent measurement of their enzymatic activities. We generated a mutant of NAT8L, exchanging aspartate 165 to alanine, which is described as having no residual enzymatic activity (24), and used this mutated construct to study the effects upon its overexpression. Although we reached a 7-fold increased expression of the mutated enzyme in iBACs (Fig. 6*A*), we observed no changes in the expression of adipogenic marker genes (Fig. 6*A*) and no impact on cellular lipid content or glycerol/FFA release (Fig. 6, *B* and *C*, unstimulated and isoproterenol-stimulated). Thus, we conclude that the enzymatic activity of NAT8L is required for its function in brown adipocytes.

Nat8l Silencing in iBACs and Knock-out of Nat8l in Mice Lead to Compensatory Up-regulation of ATP-Citrate Lyase—To analyze the influence of *Nat8l* knockdown on lipid and energy metabolism in brown fat cells, we generated iBACs stably silenced for *Nat8l*. Although various clonal populations were tested, *Nat8l* silencing efficiency did not exceed 50% (Fig. 7, *A* and *F*). Although *Nat8l* silencing in iBACs did not affect differentiation, as shown by cellular TG content (Fig. 7*D*) and neutral lipid synthesis (Fig. 7*B*), lipolysis was significantly increased in basal and isoproterenol-stimulated conditions, as reflected by increased FFA and glycerol release at day 7 when compared with control cells (Fig. 7, *D* and *E*). Additionally, the

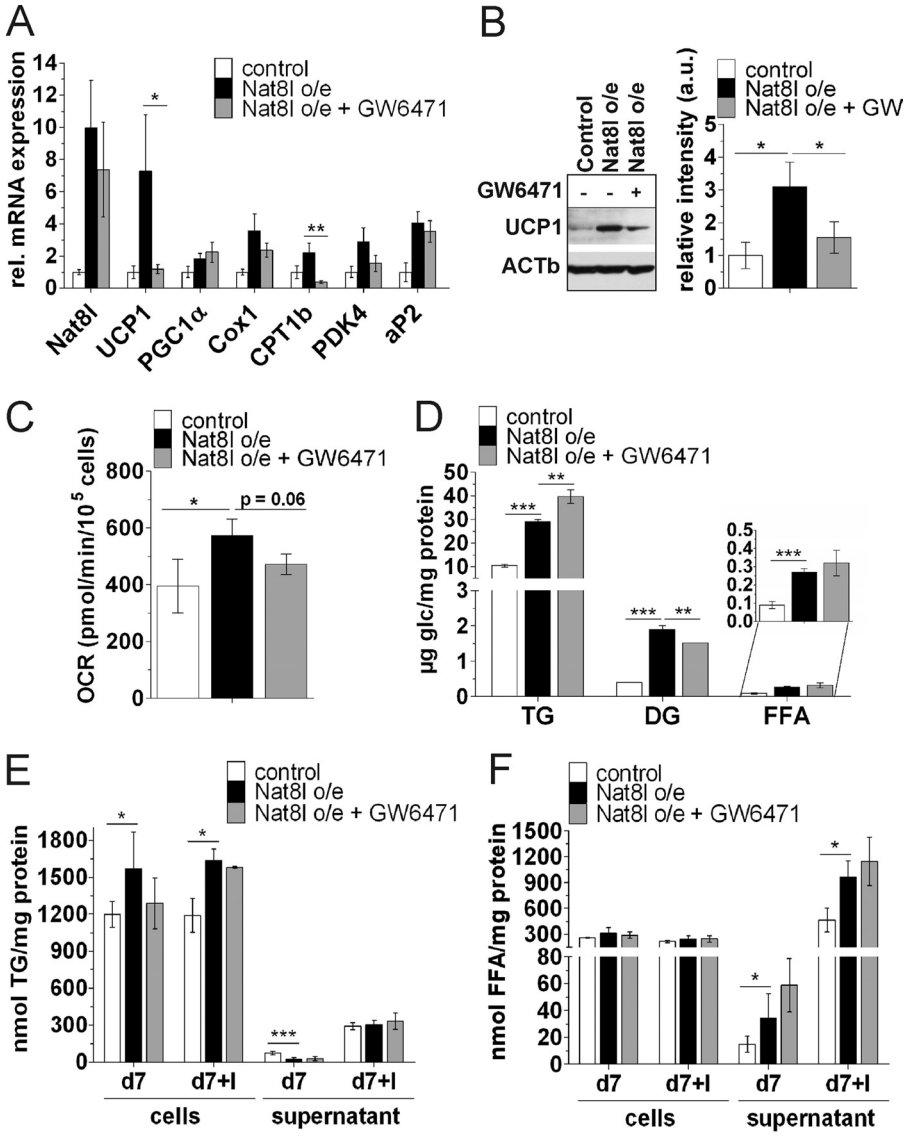

FIGURE 5. ***Nat8l*-mediated induction of *Ucp1* mRNA and oxygen consumption is PPARα-dependent, whereas lipid turnover is not.** iBACs were incubated with a 10 μM concentration of the PPARα antagonist GW6471 from day 4 until day 7 of differentiation. All experiments were performed with day 7 cells. *A*, mRNA expression of adipogenic marker genes (*aP2*, *Ucp1*, and *Pgc1α*) and genes involved in mitochondrial oxidative phosphorylation (*Cox1*) and β-oxidation (*Cpt1b* and *Pdk4*) ($n = 3$). *B*, UCP1 protein expression. One representative blot of $n = 3$ is shown. Relative band intensity is calculated from $n = 3$ and normalized to β-ACTIN. *C*, OCR measured with the Seahorse extracellular flux analyzer ($n = 3$). *D*, incorporation of [^{14}C]glucose into neutral lipids ($n = 3$). Shown are TG content (*E*) and fatty acid content (*F*) in cell lysates and supernatants of cells with and without isoproterenol treatment (10 μM for 4 h; +*I*) ($n \geq 3$). All data are presented as means ± S.D. (*error bars*), two-tailed Student's *t* test. *, $p < 0.05$; **, $p < 0.01$; ***, $p < 0.001$.

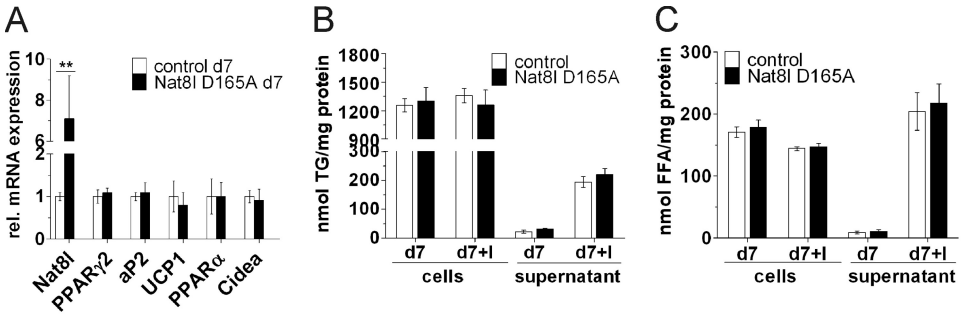

FIGURE 6. **Enzymatic activity is required for the function of *Nat8l* in brown adipocytes.** iBACs were infected with retroviral particles harboring a *Nat8l* coding sequence for producing the enzymatically inactive D165A mutant of the NAT8L protein or an empty vector as control. Cells were differentiated, and all experiments were performed with day 7 cells. *A*, mRNA expression of general (*Pparγ2* and *aP2*) and brown adipogenic genes (*Ucp1*, *Ppara*, and *Cidea*) ($n = 3$). Shown are TG content (*B*) and fatty acid content (*C*) in cell lysates and supernatants of cells with and without isoproterenol treatment (10 μM for 4 h; +*I*) ($n = 3$). All data are presented as means ± S.D. (*error bars*), two-tailed Student's *t* test. **, $p < 0.01$.

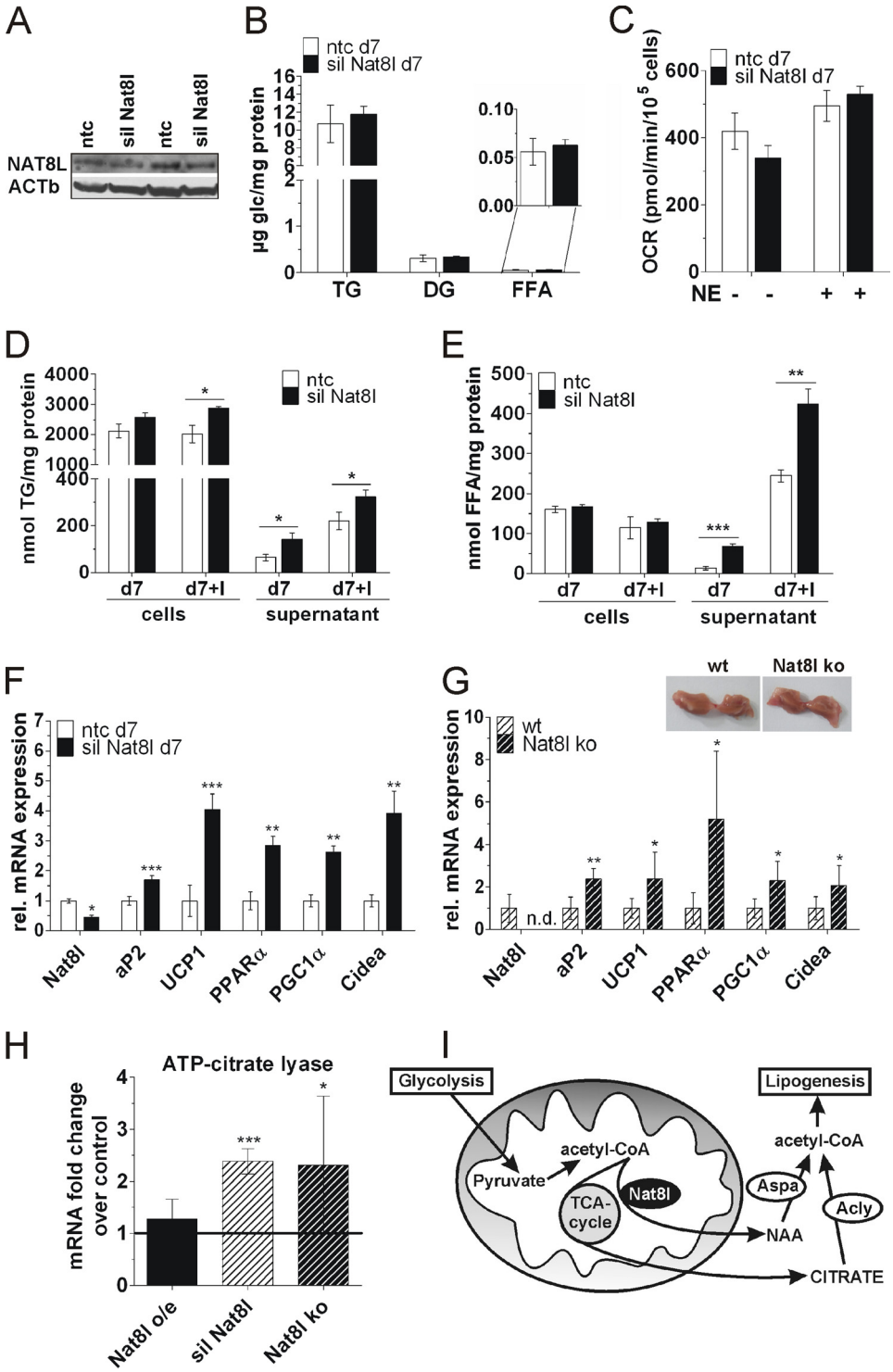

FIGURE 7. ***Nat8l* silencing in iBACs and knock-out of *Nat8l* in mice.** iBACs were infected with lentiviral particles coding for *Nat8l* shRNA (*sil Nat8l*) or using a non-target shRNA as control (*ntc*). If not otherwise stated, cells were differentiated, and all experiments were performed on day 7 (*d7*). *Nat8*-knock-out (*Nat8l KO*) and control mice (*WT*) were fed *ad libitum*, and tissues were harvested at the age of 3–4 months. *A*, protein expression of *Nat8l* in day 3 iBACs. β-actin (*ACTb*) served as a loading control. ($n = 2$). *B*, incorporation of [^{14}C]glucose into neutral lipids. ($n = 3$). *C*, OCR measured with the Seahorse extracellular flux analyzer ($n = 3$). Shown are TG content (*D*) and fatty acid content (*E*) in cell lysates and supernatants of cells with and without isoproterenol treatment (10 μM for 4 h; +*I*) ($n = 3$). Shown are expression of adipogenic genes in *Nat8l*-silenced iBACs ($n = 3$) (*F*) and in *Nat8l*-KO and WT mice ($n \geq 5$) (*G*). *Inset*, pictures of BAT of *Nat8l*-KO and WT mice. *H*, ATP citrate lyase (*Acly*) mRNA expression in *Nat8l*-overexpressing iBACs ($n = 3$), *Nat8l*-silenced iBACs ($n = 3$) and BAT of *Nat8l*-KO mice ($n \geq 5$). *I*, model proposing the NAA pathway as an alternative acetate source for cytosolic acetyl-CoA production. Data are presented as means ± S.D. (*error bars*; two-tailed Student's *t* test). *, $p < 0.05$; **, $p < 0.01$; ***, $p < 0.001$.

expression of adipogenic marker genes, such as *aP2*, *Ucp1*, *Pparα*, *Pgc1α*, and *Cidea*, was significantly increased in *Nat8l*-silenced iBACs in comparison with control cells (Fig. 7*F*). However, *Nat8l*-silenced cells did not show a difference in OCR, neither under basal nor under norepinephrine-stimulated conditions (Fig. 7*C*). Because we could not reach a very strong

Nat8l silencing in iBACs, we examined BAT from *Nat8l*-knock-out mice to evaluate some of our *in vitro* data. BAT from *Nat8l*-KO and WT mice were similar in weight (0.13 ± 0.04 g for *Nat8l*-KO *versus* 0.12 ± 0.06 g for WT mice, respectively; $n = 3$) and gross anatomy (Fig. 7*G*, *inset*), in agreement with our *in vitro* data showing that *Nat8l* silencing does not influence differentiation capacity. Moreover, we used *Nat8l*-KO mice to investigate the expression of several adipogenic marker genes. As seen for *Nat8l*-silenced iBACs (Fig. 7*F*), *aP2*, *Ucp1*, *Pparα*, *Pgc1α*, and *Cidea* mRNA expression was also significantly increased in our *in vivo* model (Fig. 7*G*).

Our data from *Nat8l*-overexpressing iBACs strongly suggest that NAA, the product of the enzymatic activity of NAT8L, can be used as an alternative source for lipid synthesis in adipocytes. Due to the fact that *Nat8l* silencing does not contrarily influence lipogenesis, we wondered whether another acetyl-CoA-producing pathway might be up-regulated to compensate for the decreased NAA-derived acetyl-CoA. Indeed, we found ATP-citrate lyase, the cytosolic enzyme converting citrate to acetyl-CoA and thereby linking cellular glucose catabolism and lipogenesis (33), significantly increased in both *Nat8l*-silenced iBACs and BAT of *Nat8l*-KO mice, whereas it was unchanged in *Nat8l*-overexpressing iBACs when compared with the respective controls (Fig. 7*H*). These data further strengthen our hypothesis that the NAT8L/NAA pathway acts as an alternative source to provide acetyl-CoA as a building block for lipid biosynthesis in adipocytes (Fig. 7*I*).

DISCUSSION

NAT8L is the enzyme responsible for the formation of NAA. In the brain, it has been shown that NAA acts as a transport molecule to provide acetate, which is used as a precursor for lipid synthesis (17). Here, we report that *Nat8l* is expressed not only in the brain but also to a high extent in adipose tissues, and its expression is induced during the differentiation of several murine and human white and brown adipogenic cell lines. Stable overexpression of *Nat8l* in iBACs leads to an increased brown marker gene expression, especially that of *Ucp1*, concomitant with an increased mitochondrial mass, number, and oxygen consumption. Supported by direct and indirect evidence from our data, we propose a model (see Fig. 8) that is based on a mitochondrial localization of NAT8L, as evidenced by our fractionation analyses of brown adipocytes *in vitro* and *in vivo*. However, in neurons, it is still under debate whether NAT8L is localized in mitochondria or ER (24–26). Neuronal NAT8L is described as using acetyl-CoA as a substrate to produce NAA, which is then transported to oligodendrocytes (16). There it is hydrolyzed by the activity of aspartoacylase (Aspa) to yield acetate, which can in turn be used for lipid synthesis (19). The expression portal BioGPS (34) and our unpublished data[4] reveal that Aspa is also highly expressed in BAT, arguing for the existence of the NAA pathway in this tissue. In the brain, it has been shown that NAA-derived acetate has a 3-fold higher potential to be incorporated into lipids than free acetate (35). Because we see elevated ^{14}C incorporation into lipids when providing labeled glucose, we speculate that, in brown adipocytes, glycolytic products are used by NAT8L to produce NAA. NAA delivers the acetate moiety for synthesis of cytosolic acetyl-CoA that is further used for FFA synthesis. These FFA are readily esterified to prevent lipotoxicity. Thus, an increase in *Nat8l* expression could drain acetyl-CoA from mitochondria. To maintain the mitochondrial acetyl-CoA pool, acetyl-CoA is mainly provided by decarboxylation of pyruvate via the pyruvate dehydrogenase complex or via β-oxidation of fatty acids. We suppose that glycolysis-derived pyruvate is not sufficient to compensate for acetyl-CoA drained into the NAA pathway because we see *Pdk4* up-regulated upon *Nat8l* overexpression. *Pdk4* inactivates the pyruvate dehydrogenase complex, resulting in a switch from glucose to fatty acid oxidation (36). Additionally, upon *Nat8l* overexpression, we see increased lipolysis providing FFA as substrate for β-oxidation. Concomitantly, the expression of *Fabp3* and *Cpt1b* is elevated. Both proteins have been shown to deliver FFA to mitochondrial β-oxidation in BAT (37, 38).

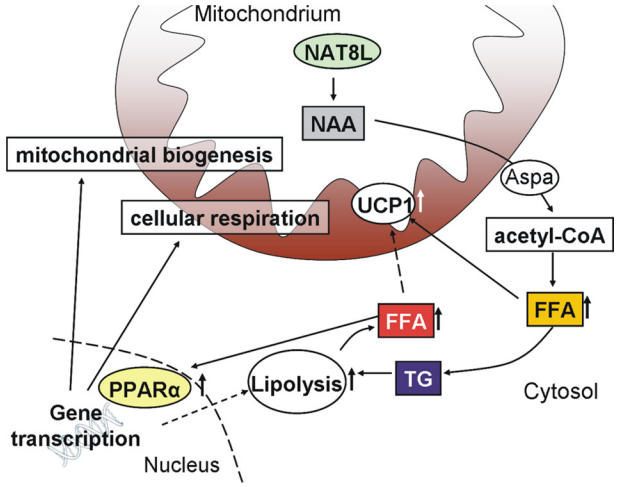

FIGURE 8. **Working model for the proposed Nat8l action in brown adipocytes as described under "Discussion."**

It is known that fatty acids and their derivatives are crucial for the activation of PPARα and UCP1 (9, 30, 39–41) and that sustained activation of PPARα increases β-oxidation (42). Recently, Ahmadian *et al.* (9) showed that lipolysis via adipose triglyceride lipase plays an essential role in maintaining adaptive thermogenesis in BAT. Together with the results of Haemmerle *et al.* (40) in cardiac muscle, this substantiates that lipolytic action is required for PPARα activation. PPARα, together with PGC1α, induces *Ucp1* expression (32). Therefore, the massive increase in *Ucp1* expression in *Nat8l*-overexpressing cells could be explained by a prominent PPARα activation by elevated lipolysis-derived FFA. Using the PPARα antagonist GW6471, we found that the *Nat8l*-induced UCP1 expression and the concomitant OCR increase were diminished to control cell levels, indicating that it is indeed a PPARα-mediated mechanism. However, increased lipogenesis and FFA release are retained during GW6471 treatment. The fact that *Nat8l* levels are still high in this condition (Fig. 5*A*) argues for a dissociation of PPARα-mediated effects and NAA-mediated lipid turnover in adipocytes. Hence, delivery of acetyl-CoA via NAT8L-mediated NAA seems to be upstream of PPARα-related effects. Moreover, our studies using the enzymatically inactive protein

[4] A. R. Pessentheiner, H. J. Pelzmann, A. Prokesch, and J. G. Bogner-Strauss, unpublished data.

support this concept because the D165A mutant does not increase lipogenesis. PPARα, its coactivator PGC1α (43, 44), and PRDM16 (45) have been shown to be important for mitochondrial biogenesis. Elevated expression of all of these genes upon *Nat8l* overexpression could explain the increase in mitochondria in these cells. Also, other brown phenotypic marker genes, such as *Dio2* (46), *C/ebpβ* (47), and *Cidea* (48), are upregulated in *Nat8l*-overexpressing cells, rendering NAT8L as a factor to enhance "browning." This is further supported by the fact that white-specific genes, like *Retn* and *Psat1* (29), are repressed. All of the observations mentioned above are consistent with our measurement of increased basal and norepinephrine-stimulated OCR and explain why these cells have a higher metabolic rate *per se*.

Knockdown of *Nat8l* in brown adipocytes had no impact on TG content, lipogenesis, and OCR, whereas lipolysis and the expression of several adipogenic marker genes were still increased. The increased lipolysis observed upon *Nat8l* knockdown might be a mechanism to generate acetyl-CoA for energy production. Lipolysis provides fatty acids that eventually can become acetylated and are further used for β-oxidation, thereby contributing to the acetyl-CoA pool. In parallel, the FFA produced by lipolysis might also activate PPARα (9) and thus increase the expression of PPARα target genes, such as *Ucp1* and *Cidea* (49), as seen in *Nat8l*-silenced iBACs and *Nat8l*-KO mice. Most interestingly, ATP-citrate lyase was significantly increased upon *Nat8l*-silencing *in vitro* and in BAT of *Nat8l*-KO mice. ATP-citrate lyase is well described to link glucose catabolism to lipogenesis by catalyzing the production of acetyl-CoA from citrate. Thus, the increase of ATP-citrate lyase mRNA expression might present a compensatory mechanism (as outlined in Fig. 7*I*) to sustain the acetyl-CoA pool upon *Nat8l* knockdown.

Although NAT8L has been implicated in many functions in the brain (mainly in the generation of substrates for myelination), its main function in adipose tissue was unknown. We imagine that, under certain circumstances, the NAA pathway could similarly serve as an additional acetyl-CoA-metabolizing mechanism in adipocytes. Our data propose (Fig. 8) that elevating *Nat8l* expression in brown adipocytes results in increased acetyl-CoA flux via the NAA pathway and concomitant higher cytoplasmic FFA anabolism, resulting in elevated TG synthesis. A parallel increase in lipolysis followed by an activation of β-oxidation can then restore acetyl-CoA back to the mitochondria. This "futile" cycle may result in increased lipid turnover and raise the oxidative potential of the brown fat cell and thereby boost the brown adipogenic phenotype. However, it remains to be seen which physiological stimuli are contributing to the regulation of the NAA pathway.

Acknowledgments—iBACs were kindly provided by Patrick Seale. We acknowledge the technical assistance provided by Corina Madreiter, Florian Stoeger, Thomas Schreiner, and Claudia Gaug. We thank Rudolf Zechner for critically reviewing the manuscript and for fruitful discussions.

REFERENCES

1. Zimmermann, R., Strauss, J. G., Haemmerle, G., Schoiswohl, G., Birner-Gruenberger, R., Riederer, M., Lass, A., Neuberger, G., Eisenhaber, F., Hermetter, A., and Zechner, R. (2004) Fat mobilization in adipose tissue is promoted by adipose triglyceride lipase. *Science* **306,** 1383–1386
2. Haemmerle, G., Zimmermann, R., Strauss, J. G., Kratky, D., Riederer, M., Knipping, G., and Zechner, R. (2002) Hormone-sensitive lipase deficiency in mice changes the plasma lipid profile by affecting the tissue-specific expression pattern of lipoprotein lipase in adipose tissue and muscle. *J. Biol. Chem.* **277,** 12946–12952
3. Cannon, B., and Nedergaard, J. (2004) Brown adipose tissue. Function and physiological significance. *Physiol. Rev.* **84,** 277–359
4. Nedergaard, J., Bengtsson, T., and Cannon, B. (2007) Unexpected evidence for active brown adipose tissue in adult humans. *Am. J. Physiol. Endocrinol. Metab.* **293,** E444–E452
5. Cypess, A. M., Lehman, S., Williams, G., Tal, I., Rodman, D., Goldfine, A. B., Kuo, F. C., Palmer, E. L., Tseng, Y.-H., Doria, A., Kolodny, G. M., and Kahn, C. R. (2009) Identification and importance of brown adipose tissue in adult humans. *N. Engl. J. Med.* **360,** 1509–1517
6. Virtanen, K. A., Lidell, M. E., Orava, J., Heglind, M., Westergren, R., Niemi, T., Taittonen, M., Laine, J., Savisto, N.-J., Enerbäck, S., and Nuutila, P. (2009) Functional brown adipose tissue in healthy adults. *N. Engl. J. Med.* **360,** 1518–1525
7. van Marken Lichtenbelt, W. D., Vanhommerig, J. W., Smulders, N. M., Drossaerts, J. M., Kemerink, G. J., Bouvy, N. D., Schrauwen, P., and Teule, G. J. (2009) Cold-activated brown adipose tissue in healthy men. *N. Engl. J. Med.* **360,** 1500–1508
8. Boss, O., and Farmer, S. R. (2012) Recruitment of brown adipose tissue as a therapy for obesity-associated diseases. *Front. Endocrinol.* (*Lausanne*) **3,** 14
9. Ahmadian, M., Abbott, M. J., Tang, T., Hudak, C. S., Kim, Y., Bruss, M., Hellerstein, M. K., Lee, H.-Y., Samuel, V. T., Shulman, G. I., Wang, Y., Duncan, R. E., Kang, C., and Sul, H. S. (2011) Desnutrin/ATGL is regulated by AMPK and is required for a brown adipose phenotype. *Cell Metab.* **13,** 739–748
10. Bartelt, A., Bruns, O. T., Reimer, R., Hohenberg, H., Ittrich, H., Peldschus, K., Kaul, M. G., Tromsdorf, U. I., Weller, H., Waurisch, C., Eychmüller, A., Gordts, P. L., Rinninger, F., Bruegelmann, K., Freund, B., Nielsen, P., Merkel, M., and Heeren, J. (2011) Brown adipose tissue activity controls triglyceride clearance. *Nat. Med.* **17,** 200–205
11. Ma, S. W., and Foster, D. O. (1986) Uptake of glucose and release of fatty acids and glycerol by rat brown adipose tissue *in vivo*. *Can. J. Physiol. Pharmacol.* **64,** 609–614
12. Darnley, A. C., Carpenter, C. A., and Saggerson, E. D. (1988) Changes in activities of some enzymes of glycerolipid synthesis in brown adipose tissue of cold-acclimated rats. *Biochem. J.* **253,** 351–355
13. Pinent, M., Hackl, H., Burkard, T. R., Prokesch, A., Papak, C., Scheideler, M., Hämmerle, G., Zechner, R., Trajanoski, Z., and Strauss, J. G. (2008) Differential transcriptional modulation of biological processes in adipocyte triglyceride lipase and hormone-sensitive lipase-deficient mice. *Genomics* **92,** 26–32
14. Wiame, E., Tyteca, D., Pierrot, N., Collard, F., Amyere, M., Noel, G., Desmedt, J., Nassogne, M.-C., Vikkula, M., Octave, J.-N., Vincent, M.-F., Courtoy, P. J., Boltshauser, E., and van Schaftingen, E. (2010) Molecular identification of aspartate *N*-acetyltransferase and its mutation in hypoacetylaspartia. *Biochem. J.* **425,** 127–136
15. Ariyannur, P. S., Moffett, J. R., Manickam, P., Pattabiraman, N., Arun, P., Nitta, A., Nabeshima, T., Madhavarao, C. N., and Namboodiri, A. M. (2010) Methamphetamine-induced neuronal protein NAT8L is the NAA biosynthetic enzyme. Implications for specialized acetyl coenzyme A metabolism in the CNS. *Brain Res.* **1335,** 1–13
16. Chakraborty, G., Mekala, P., Yahya, D., Wu, G., and Ledeen, R. W. (2001) Intraneuronal *N*-acetylaspartate supplies acetyl groups for myelin lipid synthesis. Evidence for myelin-associated aspartoacylase. *J. Neurochem.* **78,** 736–745
17. Mehta, V., and Namboodiri, M. A. (1995) *N*-Acetylaspartate as an acetyl source in the nervous system. *Brain Res. Mol. Brain Res.* **31,** 151–157
18. Burlina, A. P., Schmitt, B., Engelke, U., Wevers, R. A., Burlina, A. B., and Boltshauser, E. (2006) Hypoacetylaspartia. Clinical and biochemical follow-up of a patient. *Adv. Exp. Med. Biol.* **576,** 283–287; discussion 361–363

19. Madhavarao, C. N., Arun, P., Moffett, J. R., Szucs, S., Surendran, S., Matalon, R., Garbern, J., Hristova, D., Johnson, A., Jiang, W., and Namboodiri, M. A. (2005) Defective *N*-acetylaspartate catabolism reduces brain acetate levels and myelin lipid synthesis in Canavan's disease. *Proc. Natl. Acad. Sci. U.S.A.* **102,** 5221–5226
20. Bogner-Strauss, J. G., Prokesch, A., Sanchez-Cabo, F., Rieder, D., Hackl, H., Duszka, K., Krogsdam, A., Di Camillo, B., Walenta, E., Klatzer, A., Lass, A., Pinent, M., Wong, W.-C., Eisenhaber, F., and Trajanoski, Z. (2010) Reconstruction of gene association network reveals a transmembrane protein required for adipogenesis and targeted by PPARγ. *Cell. Mol. Life Sci.* **67,** 4049–4064
21. Furukawa-Hibi, Y., Nitta, A., Fukumitsu, H., Somiya, H., Toriumi, K., Furukawa, S., Nabeshima, T., and Yamada, K. (2012) Absence of SHATI/Nat8l reduces social interaction in mice. *Neurosci. Lett.* **526,** 79–84
22. Frezza, C., Cipolat, S., and Scorrano, L. (2007) Organelle isolation: functional mitochondria from mouse liver, muscle and cultured fibroblasts. *Nat. Protoc.* **2,** 287–295
23. Aflaki, E., Radovic, B., Chandak, P. G., Kolb, D., Eisenberg, T., Ring, J., Fertschai, I., Uellen, A., Wolinski, H., Kohlwein, S.-D., Zechner, R., Levak-Frank, S., Sattler, W., Graier, W. F., Malli, R., Madeo, F., and Kratky, D. (2011) Triacylglycerol accumulation activates the mitochondrial apoptosis pathway in macrophages. *J. Biol. Chem.* **286,** 7418–7428
24. Tahay, G., Wiame, E., Tyteca, D., Courtoy, P. J., and Van Schaftingen, E. (2012) Determinants of the enzymatic activity and the subcellular localization of aspartate *N*-acetyltransferase. *Biochem. J.* **441,** 105–112
25. Ariyannur, P. S., Madhavarao, C. N., and Namboodiri, A. M. (2008) *N*-Acetylaspartate synthesis in the brain. Mitochondria *vs*. microsomes. *Brain Res.* **1227,** 34–41
26. Lu, Z.-H., Chakraborty, G., Ledeen, R. W., Yahya, D., and Wu, G. (2004) N-Acetylaspartate synthase is bimodally expressed in microsomes and mitochondria of brain. *Brain Res. Mol. Brain Res.* **122,** 71–78
27. Pendergrass, W., Wolf, N., and Poot, M. (2004) Efficacy of MitoTracker Green and CMXrosamine to measure changes in mitochondrial membrane potentials in living cells and tissues. *Cytometry A* **61,** 162–169
28. Keij, J. F., Bell-Prince, C., and Steinkamp, J. A. (2000) Staining of mitochondrial membranes with 10-nonyl acridine orange, MitoFluor Green, and MitoTracker Green is affected by mitochondrial membrane potential altering drugs. *Cytometry* **39,** 203–210
29. Seale, P., Kajimura, S., Yang, W., Chin, S., Rohas, L. M., Uldry, M., Tavernier, G., Langin, D., and Spiegelman, B. M. (2007) Transcriptional control of brown fat determination by PRDM16. *Cell Metab.* **6,** 38–54
30. Mottillo, E. P., Bloch, A. E., Leff, T., and Granneman, J. G. (2012) Lipolytic products activate peroxisome proliferator-activated receptor (PPAR) α and δ in brown adipocytes to match fatty acid oxidation with supply. *J. Biol. Chem.* **287,** 25038–25048
31. Brandt, J. M., Djouadi, F., and Kelly, D. P. (1998) Fatty acids activate transcription of the muscle carnitine palmitoyltransferase I gene in cardiac myocytes via the peroxisome proliferator-activated receptor α. *J. Biol. Chem.* **273,** 23786–23792
32. Barbera, M. J., Schluter, A., Pedraza, N., Iglesias, R., Villarroya, F., and Giralt, M. (2001) Peroxisome proliferator-activated receptor α activates transcription of the brown fat uncoupling protein-1 gene. A link between regulation of the thermogenic and lipid oxidation pathways in the brown fat cell. *J. Biol. Chem.* **276,** 1486–1493
33. Sugden, M. C., Watts, D. I., Marshall, C. E., and McCormack, J. G. (1982) Brown-adipose-tissue lipogenesis in starvation. Effects of insulin and (−)-hydroxycitrate. *Biosci. Rep.* **2,** 289–297
34. Wu, C., Macleod, I., and Su, A. I. (2013) BioGPS and MyGene.info. Organizing online, gene-centric information. *Nucleic Acids Res.* **41,** D561–565
35. D'Adamo, A. F., Jr., and Yatsu, F. M. (1966) Acetate metabolism in the nervous system. *N*-Acetyl-L-aspartic acid and the biosynthesis of brain lipids. *J. Neurochem.* **13,** 961–965
36. Zhao, G., Jeoung, N. H., Burgess, S. C., Rosaaen-Stowe, K. A., Inagaki, T., Latif, S., Shelton, J. M., McAnally, J., Bassel-Duby, R., Harris, R. A., Richardson, J. A., and Kliewer, S. A. (2008) Overexpression of pyruvate dehydrogenase kinase 4 in heart perturbs metabolism and exacerbates calcineurin-induced cardiomyopathy. *Am. J. Physiol. Heart Circ. Physiol.* **294,** H936–H943
37. Vergnes, L., Chin, R., Young, S. G., and Reue, K. (2011) Heart-type fatty acid-binding protein is essential for efficient brown adipose tissue fatty acid oxidation and cold tolerance. *J. Biol. Chem.* **286,** 380–390
38. Ji, S., You, Y., Kerner, J., Hoppel, C. L., Schoeb, T. R., Chick, W. S., Hamm, D. A., Sharer, J. D., and Wood, P. A. (2008) Homozygous carnitine palmitoyltransferase 1b (muscle isoform) deficiency is lethal in the mouse. *Mol. Genet. Metab.* **93,** 314–322
39. Fedorenko, A., Lishko, P. V., and Kirichok, Y. (2012) Mechanism of fatty-acid-dependent UCP1 uncoupling in brown fat mitochondria. *Cell* **151,** 400–413
40. Haemmerle, G., Moustafa, T., Woelkart, G., Büttner, S., Schmidt, A., van de Weijer, T., Hesselink, M., Jaeger, D., Kienesberger, P. C., Zierler, K., Schreiber, R., Eichmann, T., Kolb, D., Kotzbeck, P., Schweiger, M., Kumari, M., Eder, S., Schoiswohl, G., Wongsiriroj, N., Pollak, N. M., Radner, F. P., Preiss-Landl, K., Kolbe, T., Rülicke, T., Pieske, B., Trauner, M., Lass, A., Zimmermann, R., Hoefler, G., Cinti, S., Kershaw, E. E., Schrauwen, P., Madeo, F., Mayer, B., and Zechner, R. (2011) ATGL-mediated fat catabolism regulates cardiac mitochondrial function via PPAR-α and PGC-1. *Nat. Med.* **17,** 1076–1085
41. Chakravarthy, M. V., Lodhi, I. J., Yin, L., Malapaka, R. R., Xu, H. E., Turk, J., and Semenkovich, C. F. (2009) Identification of a physiologically relevant endogenous ligand for PPARα in liver. *Cell* **138,** 476–488
42. Huang, J., Jia, Y., Fu, T., Viswakarma, N., Bai, L., Rao, M. S., Zhu, Y., Borensztajn, J., and Reddy, J. K. (2012) Sustained activation of PPARα by endogenous ligands increases hepatic fatty acid oxidation and prevents obesity in ob/ob mice. *FASEB J.* **26,** 628–638
43. Puigserver, P., Wu, Z., Park, C. W., Graves, R., Wright, M., and Spiegelman, B. M. (1998) A cold-inducible coactivator of nuclear receptors linked to adaptive thermogenesis. *Cell* **92,** 829–839
44. Wu, Z., Puigserver, P., Andersson, U., Zhang, C., Adelmant, G., Mootha, V., Troy, A., Cinti, S., Lowell, B., Scarpulla, R. C., and Spiegelman, B. M. (1999) Mechanisms controlling mitochondrial biogenesis and respiration through the thermogenic coactivator PGC-1. *Cell* **98,** 115–124
45. Murholm, M., Dixen, K., Qvortrup, K., Hansen, L. H., Amri, E.-Z., Madsen, L., Barbatelli, G., Quistorff, B., and Hansen, J. B. (2009) Dynamic regulation of genes involved in mitochondrial DNA replication and transcription during mouse brown fat cell differentiation and recruitment. *PLoS One* **4,** e8458
46. de Jesus, L. A., Carvalho, S. D., Ribeiro, M. O., Schneider, M., Kim, S. W., Harney, J. W., Larsen, P. R., and Bianco, A. C. (2001) The type 2 iodothyronine deiodinase is essential for adaptive thermogenesis in brown adipose tissue. *J. Clin. Invest.* **108,** 1379–1385
47. Carmona, M. C., Hondares, E., Rodríguez de la Concepción, M. L., Rodríguez-Sureda, V., Peinado-Onsurbe, J., Poli, V., Iglesias, R., Villarroya, F., and Giralt, M. (2005) Defective thermoregulation, impaired lipid metabolism, but preserved adrenergic induction of gene expression in brown fat of mice lacking C/EBPβ. *Biochem. J.* **389,** 47–56
48. Li, P. (2004) Cidea, brown fat and obesity. *Mech. Ageing Dev.* **125,** 337–338
49. Viswakarma, N., Yu, S., Naik, S., Kashireddy, P., Matsumoto, K., Sarkar, J., Surapureddi, S., Jia, Y., Rao, M. S., and Reddy, J. K. (2007) Transcriptional regulation of Cidea, mitochondrial cell death-inducing DNA fragmentation factor α-like effector A, in mouse liver by peroxisome proliferator-activated receptor α and γ. *J. Biol. Chem.* **282,** 18613–18624